Numerical analysis of microring resonator obtained by wafer-bonding technology

Mihai Kusko*[1], Dimitris Alexandropoulos[2], C. W. Tee[3], Alexandros Kapsalis[2], Dana Cristea[1], Dimitris Syvridis[2], Cristian Kusko[1]

1. National Institute for R&D in Microtechnologies (IMT-Bucharest) Laboratory of Microphotonics. PO Box 38-160, Bucharest 023573, Romania
e-mail: mihaik@imt.ro. phone: +40.21.490 84 12; fax: +40.21.490 82 38

2. Optical Communications Laboratory,Department of Informatics and Telecommunications. University Of Athens. Panepistimiopolis, Ilissia, AthensGR 157 84, Greece.

3. Centre for Photonic Systems, University of Cambridge, Wiliam Gates Buiding, 15 JJ Thomson Avenue, Cambridge CB3 0FD, United Kingdom

ABSTRACT

Microring resonators will be one of the most important components of the next generation of optical communications. In this work, we have analyzed from theoretical perspective a new proposed microring resonator structure based on the wafer-bonding technique which implies the vertical coupling between the passive bus waveguide and the active ring resonator. We have investigated the possibility to obtain the monomode operation of the active ring waveguide for certain ring radius values by the selective attenuations of the higher order modes and the obtaining of the desired coupling efficiency by varying the technological parameters like the layers thickness, etching depth, bus waveguide width and the offset (misalignment between the ring and the bus waveguide). Depending on the fabrication method, the misalignment between the ring resonator and the bus waveguide may vary within a significant range. Therefore, we considered a much wider bus waveguide in the coupling region in order to minimise the effects of misalignment.

Keywords. Microring resonators, modeling,

1. INTRODUCTION

Recently, optical micro-ring resonators have received considerable attention since they provide a promising route towards very large-scale-integrated photonics. The versatility of these elements is appreciated by the research community and .already there have been many accounts of the application of micro-ring resonators as the building blocks for many applications in optical signal processing and optical communication [1, 2]. The microring structures can be fabricated in two basic configurations: laterally coupled [3] and vertical coupled [4, 5]. In the former configuration, the bus waveguides and the ring waveguide are situated on the same level. Although this configuration is very simple, there are major drawbacks imposed by the very tight fabrication tolerances and the impossibility to have the ring waveguide different from the bus waveguide. The vertical coupled configuration is characterized by the possibility to have the bus waveguides and the ring waveguide at different levels, in different configurations adding an extra degree of freedom from the technological point of view. The fabrication tolerance is more relaxed for the last configuration due to the fact that the distance between the bus and the ring is determined by the thickness of the separation layer which can be technologically controlled with high accuracy. There are several methods for obtaining vertically coupled microring structures. Recently, a new type of microring structure obtained by wafer bonding was proposed [6] This type of structure is analyzed in this work from the theoretical point of view. An outline of the fabrication method is reproduced in Figure 1.

Integrated Optics: Theory and Applications, edited by Tadeusz Pustelny, Paul V. Lambeck, Christophe Gorecki, Proc. of SPIE Vol. 5956, 59561E, (2005) · 0277-786X/05/$15 · doi: 10.1117/12.623000

Downloaded from SPIE Digital Library on 03 Nov 2009 to 159.226.100.225. Terms of Use: http://spiedl.org/terms

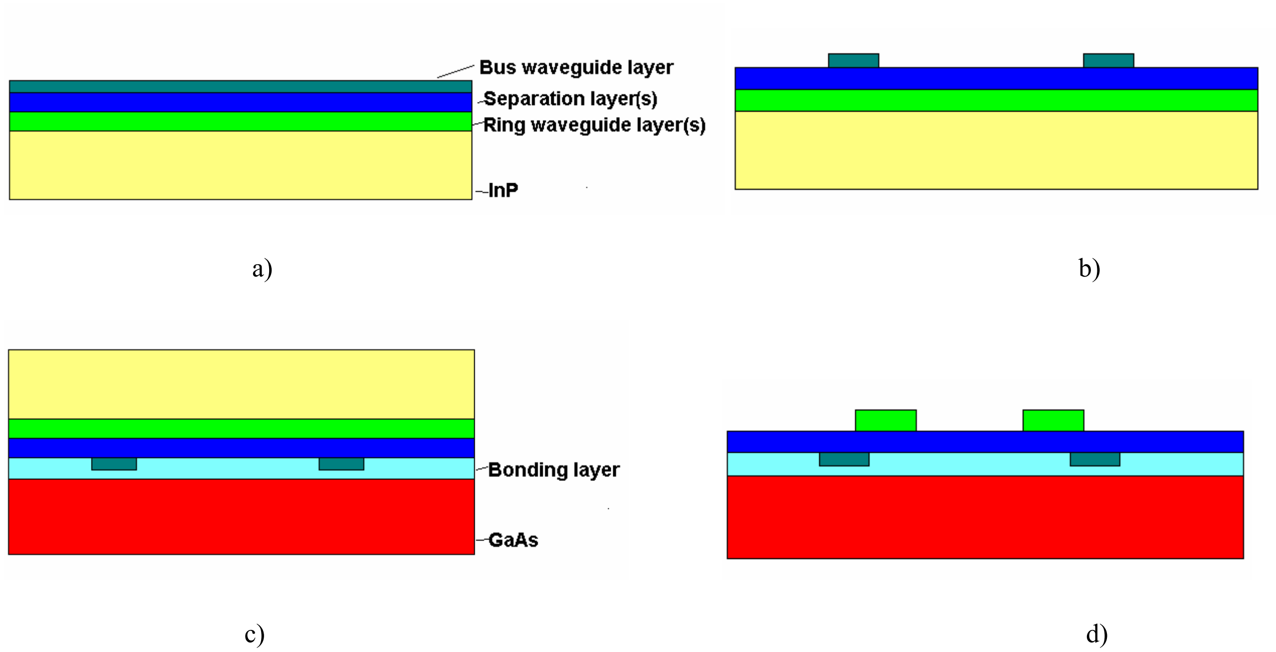

Figure 1. An outline of fabrication method. a) Epitaxial growth of layers. b) Bus waveguide patterning. c) wafer bonding process. d) ring waveguide patterning.

In the following we propose and describe two alternatives for the design of quasi-single-mode passive micro-ring structures. In both cases the layers of the structure are modified so that either the coupling to higher modes is suppressed or in the case of the excitation of higher order modes the loss properties of the structure are tailored so that these are selectively attenuated.

2. DESIGN

A very powerful method for the numerical simulation of the ring resonators is the Finite Difference Time Domain (FDTD) . This method consists in the discretisation of the Maxwell equations taking into account the appropriate boundary conditions. This is a highly intensive numerical method and yields the rigorous electromagnetic field configurations for any two-dimensional (2D) or three-dimensional (3D) [7] structure. However for large 3D ring-bus configurations (e.g. R=20 μm) this technique becomes prohibitive due to the very high memory usage and long computation times. It is advantageous to use a combination of numerical methods and analytical approaches for the description of the light propagation in a circular resonator. One of these approaches is the scattering matrix method where one can use the coupling coefficients numerically computed (for instance with FDTD method) in order to calculate the overall spectral characteristic of the resonator. This method has been extensively treated in the literature [8, 9].

The degrees of freedom in the design are the lateral offset, the thickness and the composition of the layers and their widths. All these factors have a combined effect on the functional properties of the structure, and therefore a rigorous numerical analysis taking into account all these parameters is required.

The lateral offset represents the misalignment of the ring waveguide with respect to the bus waveguide; this is illustrated in figure 2. It quantifies the extent of the perturbation the bus induces to the ring field distribution and vice versa. Offset is considered positive when the ring waveguide center and bus waveguide center are not intersecting. The offset value

Downloaded from SPIE Digital Library on 03 Nov 2009 to 159.226.100.225. Terms of Use: http://spiedl.org/terms

tunes the power coupling efficiency; this can be intentional or accidental. The former presupposes very good control of the growth and wafer bonding process while the latter suggests fabrication tolerance dependent operation.

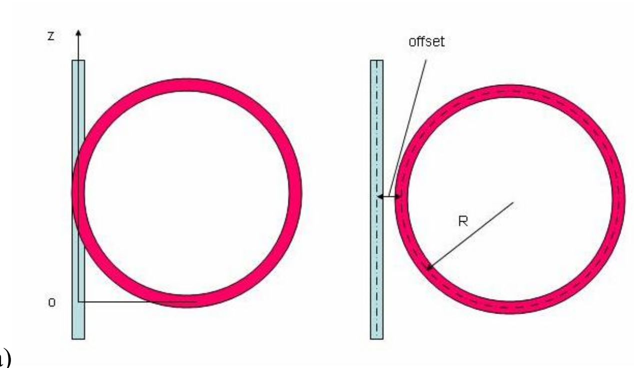

a)

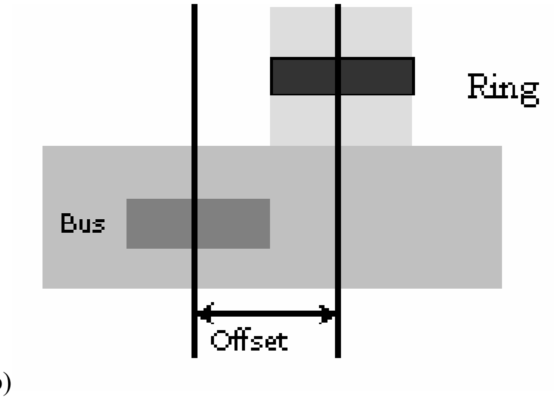

b)

Figure 2. a) Schematic diagram of the ring-bus alignment showing the offset. b) Cross section of the micro-ring

A straightforward way for ensuring single-mode operation of the ring waveguide is to design a ring waveguide that supports only the fundamental mode. In our case the ring waveguide width is quite large and the refractive index contrast between silicon nitride cladding (n = 1.84) and InGaAsP or InP materials used in the ring waveguide fabrication is high enough causing the existence of the higher order modes.

This approach consists in designing a ring waveguide structure which allows the selective attenuation of the higher order modes for a certain ring radius range. In order to eliminate the influence of the higher order ring modes upon the device operation it is necessary to have an almost complete extinction of these modes before a half-cycle run ($L = \pi R$, where R represents the ring radius). This distance is accounted if the microring resonator device has two bus waveguides. If the microring resonator device has only a bus waveguide, the distance required for eliminating the higher orders modes becomes $L = 2 \pi R$. The ring curvature that induces the propagation losses of the higher order modes affects the fundamental mode too. That is why we have to find a compromise in order to minimize the losses of the fundamental mode. The configuration of the passive vertically integrated microring resonator is given in Figure 3 and table 1. The ring is passivated with a SiNx layer (n = 1.84). The bus rib is covered with a SiOs/SiNx layer (pasivation and planarization). The ring waveguide and bus waveguide width is 1.8 μm. This rather large width value is necessary for maintaining acceptable tolerance fabrication.

The increased propagation losses of the higher order modes of the ring appear due to the high-index slab layer (n = 3.30) with 300 nm thickness, that allows the radiation carried by the higher order modes to escape from the ring., The ring core thickness has been chosen so that the fundamental mode is not very lossy. The optimum layer configuration is given in the table 1.

Downloaded from SPIE Digital Library on 03 Nov 2009 to 159.226.100.225. Terms of Use: http://spiedl.org/terms

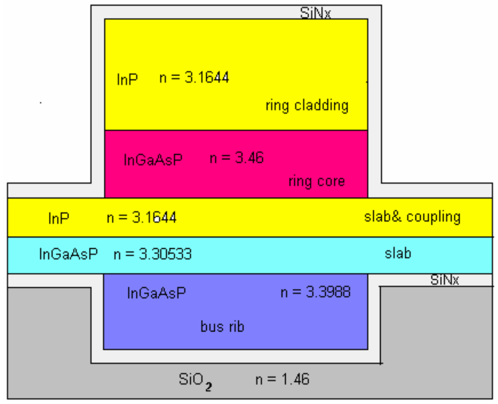

Figure 3. Proposed structure for selective attenuation of the higher order ring modes.

Layer	Material	Refractive index	Thickness [nm]	Role
1	InP	3.16	1500	Ring cladding
2	InGaAsP	3.46	280	Ring core
3	InP	3.16	350	Slab coupling
4	InGaAsP	3.30	300	slab
4a	InP	3.16	20	Etch stop (neglected in simulation)
5.	InGaAsP	3.39	400	Bus rib

Table 1. Layer configuration for the vertical coupled microring resonator

An alternative approach to the selective attenuation of the higher order modes for the design of passive micro-ring structures is discussed in the following. It is possible to ensure single-mode operation and at the same time relax fabrication tolerances by tailoring the geometrical characteristics of the bus and ring waveguide so that the effective index of the bus waveguide is always higher than that of the ring. In this way, the phase matching conditions favour the coupling of the fundamental mode of the bus to the fundamental mode of the ring, while retaining at the same time acceptable values of the coupling coefficient.

A schematic diagram of the proposed structure is shown in figure 4. We identify the following characteristics; the bus and the ring waveguides are made of $In_{1-x}Ga_xAs_yP_{1-y}$ layers. The InP layer plays the role of the slab waveguide, while another InP layer (ring rib) is placed between the initial InP layer (slab coupling) and the ring waveguide. The purpose of these layers is threefold; the use of InP, instead of the InGaAsP is to suppress the coupling of bus modes to the slab, which acts as a drain of radiation. This is possible because of the higher refractive index difference between the bus waveguide (InGaAsP) and the slab waveguide (InP). The InP layers, slab and ring rib, can also be used as control for tuning the coupling efficiency, by varying the thickness.

Downloaded from SPIE Digital Library on 03 Nov 2009 to 159.226.100.225. Terms of Use: http://spiedl.org/terms

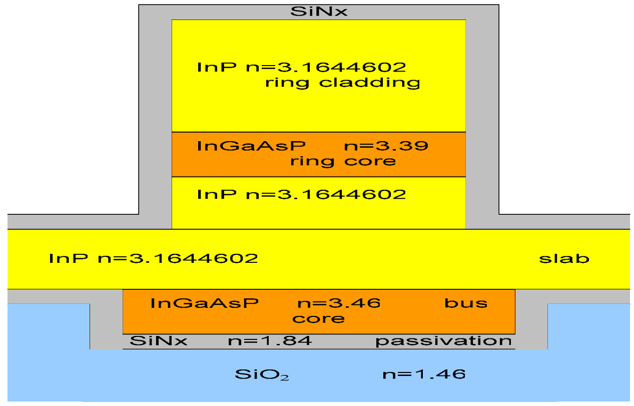

Figure 4. Proposed structure for selective excitation of the fundamental mode.

The underline idea of the proposed scheme is the manipulation of the effective indices so as to achieve a higher refractive index for the bus fundamental mode than the ring fundamental mode. We first produce the mapping of the effective refractive index of the fundamental mode of the ring and bus waveguides.

Fig. 5 shows the variation of n_{eff} of the ring against ring waveguide thickness for three radii. The radii are chosen on the grounds of FSR and dynamic performance of potential devices. The usual trend is exhibited; i.e. increasing n_{eff} with ring thickness and with decreasing R.

In Fig. 6 the n_{eff} bus waveguide is plotted against bus thickness for various values of widths. The effective index increases with the thickness and width, although the influence of the width is much smaller than the influence of the thickness.

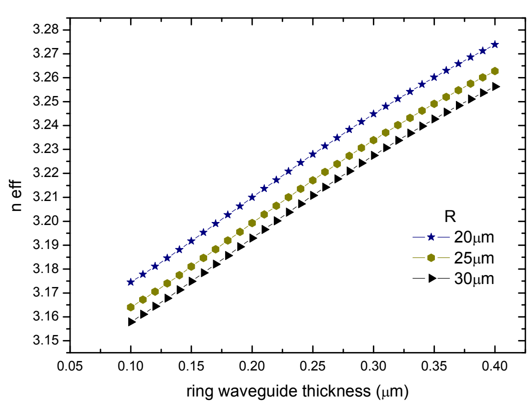

Figure 5. Ring waveguide effective refractive index of the fundamental mode versus ring thickness for various ring radii. The ring waveguide thickness is 1.8 μm.

Downloaded from SPIE Digital Library on 03 Nov 2009 to 159.226.100.225. Terms of Use: http://spiedl.org/terms

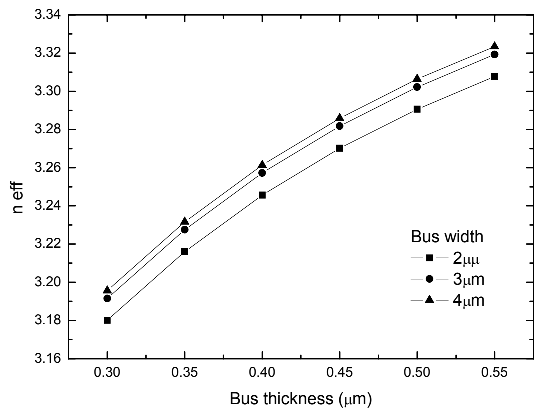

Figure 6. Bus waveguide effective refractive index of the fundamental mode versus bus thickness widths as pointed in the figure.

Figures 5 and 6 provide the necessary information for the realisation of single-mode microring structures. From these we choose three test structures to study the modal characteristics and assess the proposed design scheme. These are tabulated in tables 2 and 3.

Table 2					
layer	Description	t (μm)	n(μm)	λ_g
1	Bus	0.35 μm	3.46	1290 nm
2	InP slab&coupling	0.35μm	3.16	920 nm
3	InP ring rib	0.35 μm	3.16	920 nm
4	RING	To be defined in table 3	3.39	1200 nm
5	InP ring rib	1.5 μm	3.16	920 nm

Table 3				
	Bus	Ring		
Structure	w (μm)	w(μm)	t(μm)	R (μm)
1	2	1.8	0.17	20
2	3	1.8	0.2	20
3	4	1.8	0.22	20
4	2	1.8	0.22	30
5	3	1.8	0.24	30
6	4	1.8	0.27	30

(w: width, t: thickness, n: refractive index, R: radius, λ_g: bandgap wavelength)

The effective indices of the bus and ring waveguides can be tailored by varying their geometrical dimensions, for given material refractive indices. As a rule of thumb, increasing the dimensions, the effective index is also increased either for the bus or the ring. The increased refractive index translates to a more efficient confinement of the respective mode to the waveguide (bus or ring)

Downloaded from SPIE Digital Library on 03 Nov 2009 to 159.226.100.225. Terms of Use: http://spiedl.org/terms

Apart from the geometrical characteristics, the effective indices for a given structure can be tuned with the proper choice of compositions. It is found that it is advantageous to modify the compositions of the bus and ring waveguides in order to obtain material refractive index of 3.46 at 1550nm for the bus ($x = 0.28$, $y = 0.60$ and Eg=0.961eV) and 3.39 at 1550nm for the ring ($x = 0.22$, $y = 0.47$ Eg=1.037 eV).

For the investigation of the ring structure based on the selective attenuation approach we have analyzed the propagation losses of the ring waveguide. The losses analysis shows that the fundamental mode's attenuation after a half-cycle run is much smaller than that of the higher order modes. This is shown in Table 4 which presents the losses of the ring modes after a half-cycle run for different ring radius values. The ring width is 1.8 μm.

Mode order	Radius 20 μm	Radius 30 μm	Radius 40 μm	Radius 50 μm
0	0.3896	0.881	0.96	1
1	0	0	0.02	0.06
2	0	0	0	0
3	0.06	0.03	0.015	0
4	0	0	0	0.015
5	0.066	0.024	0.03	0.088

Table 4. Relative intensity after a half-cycle run.

The results tabulated in table 4 show that although the higher order modes are highly extinguished they are not completely eliminated. Therefore, a combination of the present approach with the one described in the previous section i.e selective coupling of the fundamental mode of the ring is needed for obtaining a single-mode operating device.

The field distribution of the fundamental modes for the radii R=20 and 50 μm are presented in Figs. 7 a- 7b.

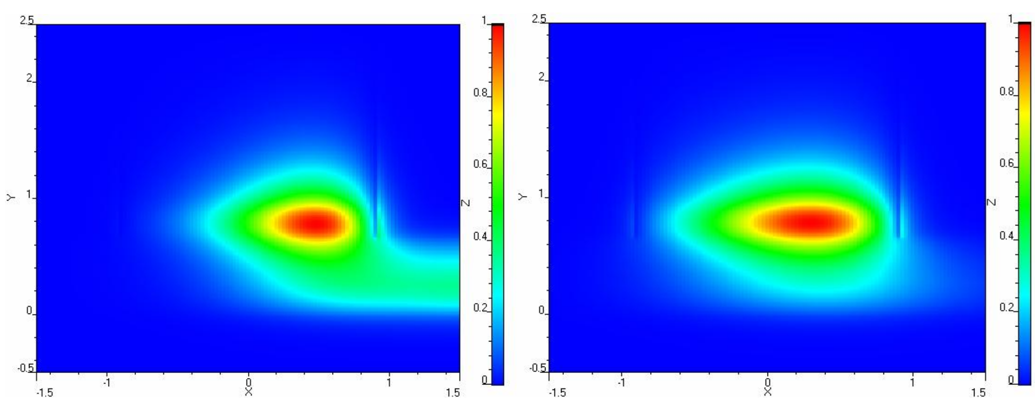

a) b)

Figure 7. TE field of the fundamental mode for the following ring radii: a)R = 20 μm b) R = 50 μm

It is noteworthy to mention that the mode field profile becomes more asymmetric as the ring radius is smaller as it can be seen in Fig 7a and 7b.

The loss analysis for the structures studied in the frame of the second approach reveals that there are insignifiant propagation losses after a half-cycle run for the fundamental mode for R=20 μm and R=30 μm. The mode field profiles for some structures are represented in Figure 8.

Downloaded from SPIE Digital Library on 03 Nov 2009 to 159.226.100.225. Terms of Use: http://spiedl.org/terms

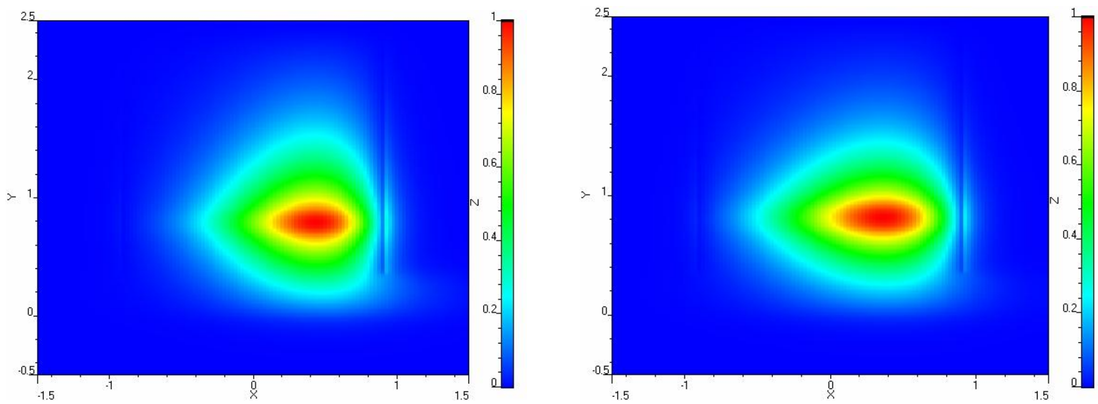

a) b)

Figure 8. TE field of the fundamental mode for the different structures. a) Structure 1; b) Structure 4.

3. COUPLING ANALYSIS

The operational characteristics of the microring devices are determined by the coupling characteristics from bus to ring waveguide. The dependence on the coupling properties is studied using the scattering matrix formalism [9]. The first structure analyzed is the structure described in Fig. 3. Due to the fact that the higher order modes of the ring waveguide are almost extinct after a half-cycle run, only the fundamental mode is considered. For the purposes of the present approach the scattering matrix describing the ring-bus system becomes a 2×2 matrix. The scattering matrix coefficients are obtained by performing the relevant overlap integrals.

As discussed previously, the offset value affects the coupling characteristics. Different offset values are considered, namely 0, 0.25, 0.5, 0.75, and 1 μm. The ring radius values are 20, 30, 40 and 50 μm. Bus-ring coupling efficiency variation with the offset and the ring radius are presented in Figure 9a. The coupling coefficients bus-ring and ring-bus of the scattering matrix decrease dramatically with offset, while the coupling efficiency has an increasing trend with the ring radius.

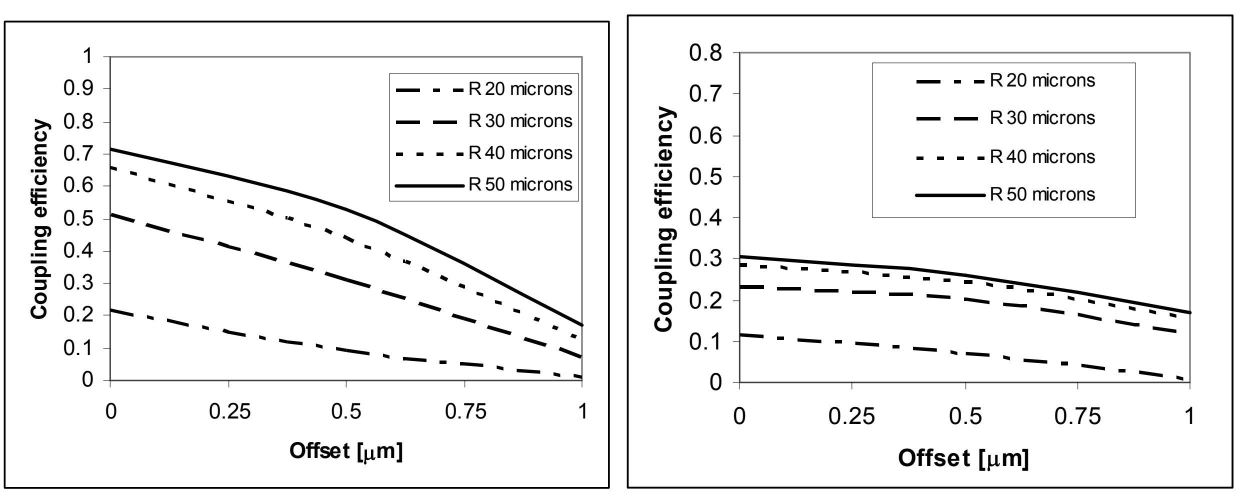

a) b)

Figure 9. Coupling efficiency from bus to ring vs. offset for different ring radius values .a) bus width 1.8 μm; b) bus width 4 μm

Downloaded from SPIE Digital Library on 03 Nov 2009 to 159.226.100.225. Terms of Use: http://spiedl.org/terms

The radiation coupling from bus to ring is represented in Figure 10. The ring radius is 40 µm and the offset value is 0.5 µm.

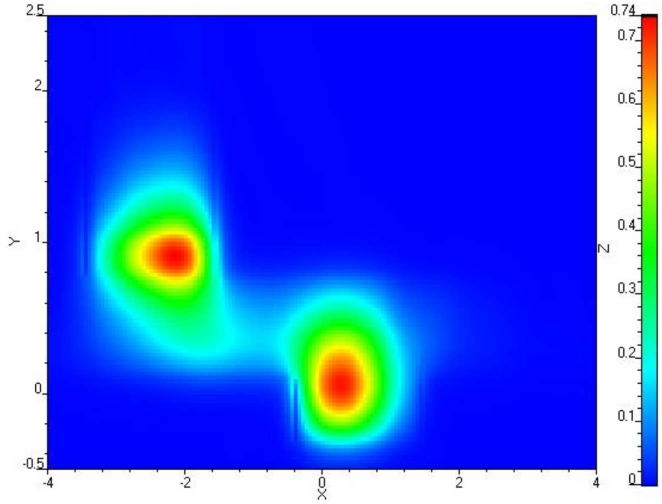

Figure 10. Radiation coupling from bus to ring. Offset 0.5 µm.

In order to minimize the offset influence, we have investigated a structure with a large bus waveguide (bus waveguide width = 4 µm). As expected, the coupling efficiency variation with offset is less pronounced (see Fig 9b). However, the coupling efficiency in the fundamental mode is lower than that obtained for the normal case.

The same analysis was performed for the structure described in the in the Fig. 4. The selective coupling of the fundamental mode of the ring can be obtained for larger positive offset values (offset > 0.5 µm). Since this behavior is also noticed for the first structure, we have concluded that a positive offset value could provide the ring fundamental mode selective coupling unless the bus waveguide effective index is much lower than the effective index of the ring fundamental mode. The radiation coupling from bus to ring is represented in Figure 11 for structure 4 (according to table 3 notation). Offset value is 0.5 µm. The field distributions represented in Figs. 10 and 11 are obtained at the end of the coupling region.

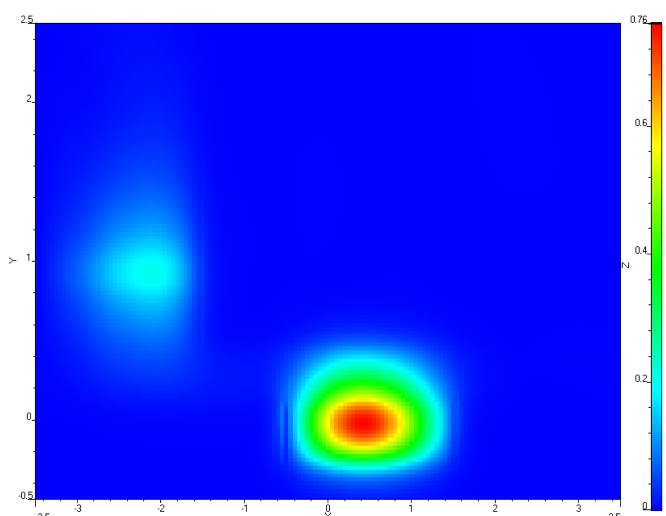

Figure 11. Radiation coupling from bus to ring –Structure 4. Offset 0.5 µm.

Downloaded from SPIE Digital Library on 03 Nov 2009 to 159.226.100.225. Terms of Use: http://spiedl.org/terms

The spectral characteristics for some structures with two bus waveguide are plotted below. The drawings are self-explanatory.

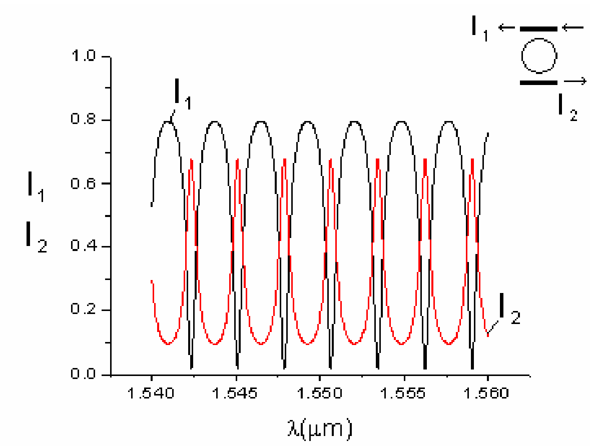

a)

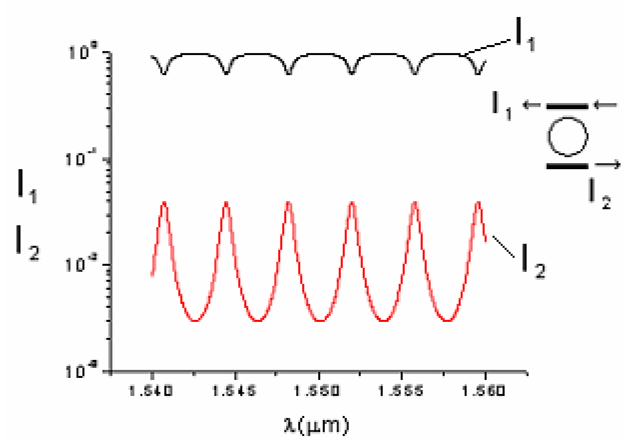

b)

Figure 12. The spectral characteristics for some structures . a) First type structure (R = 40 μm, Offset = 0.5 μm)

b) Second type structure (Structure4, Offset 0.75 μm)

4. CONCLUSIONS

In this work we have presented a detailed analysis of two different classes of single-mode operating passive microring structures.

We used two approaches for accomplishing this goal. The concept underlining the first approach consists in the selective attenuation of the higher order modes of the ring, while minimizing the losses of the fundamental mode. The second approach is based on the preferential coupling of the fundamental ring mode with the fundamental bus mode. The selective coupling can be attained by matching the effective index of the bus waveguide fundamental mode with the effective index of the ring waveguide fundamental mode.

Downloaded from SPIE Digital Library on 03 Nov 2009 to 159.226.100.225. Terms of Use: http://spiedl.org/terms

In order to design the single mode operating microring passive devices based on these two concepts we have performed a thorough and rigorous numerical investigation of various structures. The investigation included the analysis of the bus and ring modes and the dispersion of these modes as a function of the ring radius as well as the analysis of the coupling and transmission coefficients of the bus-ring coupling region as a function of the ring radius and the lateral offset.

For the first approach, this analysis reveals that for large radii (R=40μm, R=50μm) the highly order modes are almost extinguished while the fundamental mode propagates along the ring with almost zero attenuation, whereas for the smaller radii (R=20μm, R=30μm) the fundamental mode suffers a significant attenuation. The coupling analysis shows that there is a certain lateral offset for which the structure presents a single mode coupling with a high efficiency.

For the second approach, the same analysis shows that the fundamental mode presents insignifiant propagation losses propagation for the ring radius values R=20μm and R=30μm. It is noticeable that the single-mode operation for the second type of the structures is better fulfilled for offset values greater than 0.5 μm.

We have used the previously calculated coupling coefficients to calculate the spectral characteristics of the proposed structures in the framework of the scattering matrix formalism. As the lateral misalignment of the ring is the most important source of the fabrication errors, we have studied the dependence of the spectral response with respect to the lateral offset. We have found that the structures based on the first approach are tolerant to the fabrication misalignment tolerances varying up to ±0.25 μm, provided that the initial designed lateral offset value is 0.5 μm, and the structures based on the second approach are tolerant to fabrication misalignments varying up to ±0.25 μm, provided that the initial designed lateral offset value is 0.75 μm.

As a concluding remark, we note that the aforementioned results indicate that the single-mode operation can be implemented by imposing a nonzero lateral offset, a better match between the fundamental mode of the ring and bus waveguide effective indices. Because there is a little amount of power corresponding to the ring higher order modes coupled in the ring, it is better to use a structure which allows the selective attenuations in order to obtain a true single-mode operation microring resonator.

ACKNOWLEDGEMENT

This work has been supported by FP6 project Waferbonding and Active Passive Integration Technology and Implementation – WAPITI.

REFERENCES

[1] C. K. Madsen and J. H. Zhao, *Optical Filter Design and Analysis: A Signal Processing Approach*. New York: Wiley, 1999

[2] N. Hodgson and H. Weber, *Optical Resonators*. Berlin, Germany: Springer-Verlag, 1997, ch. 20.

[3] B. E. Little, S. T. Chu, H. A. Haus, J. Foresi, and J. P. Laine, "Microring resonator channel dropping filters," *J. Lightwave Technol.*, vol. 15, pp. 998–1005, June 1997.

[4] B. E. Little, S. T. Chu,W. Pan, D. Ripin, T. Kaneko, Y. Kokubun, and E. Ippen, "Vertically coupled glass microring resonator channel dropping filters," *IEEE Photon. Technol. Lett.*, vol. 11, pp. 215–217, Feb. 1999.

[5] D. V. Tishinin, P. D. Dapkus, A. E. Bond, I. Kim, C. K. Lin, and J. O'Brien, "Vertical resonant couplers with precise coupling efficiency control fabricated by wafer bonding," *IEEE Photon. Technol. Lett.*, vol. 11, pp. 1003–1005, Aug. 1999.

Downloaded from SPIE Digital Library on 03 Nov 2009 to 159.226.100.225. Terms of Use: http://spiedl.org/terms

[6] M. Hamacher, U. Troppenz, H. Heidrich, “Optically amplifying microring resonator components based on GaInAsP/InP” *CAS 2004 proceedings*, pp. 179-188.

[7] S. C. Hagness, D. Rafizadeh, S. T. Ho, and A. Taflove, “FDTD microcavity simulations: Design and experimental realization of waveguide-coupled single-mode ring and whispering-gallery-mode disk resonators,” *J. Lightwave Technol.*, vol. 15, pp. 2154–2165, Nov. 1997.

[8] Otto Schwelb*,* Transmission, Group Delay, and Dispersion in Single-Ring Optical Resonators and Add/Drop Filters—A Tutorial Overview, *J. Lightwave Technol.*, vol. 22, pp. 1380–1394, May 2004.

[9] L. Caruso, and I. Montrosset, “Analysis of a racetrack microring resonator with MMI coupler”, *IEEE J. of Lightwave Technol*., vol. 21, pp., 206- 210, 2003

Downloaded from SPIE Digital Library on 03 Nov 2009 to 159.226.100.225. Terms of Use: http://spiedl.org/terms